Spray/wall interaction in direct-injection spark ignition engines equipped with multi-hole injectors

Abo-Serie E., Gavaises M. and Arcoumanis C.

School of Engineering and Mathematical Sciences
City University London
Northampton Square
London, EC1 0HB

e.abo-serie@city.ac.uk, m.gavaises@city.ac.uk, c.arcoumanis@city.ac.uk

The spray injected from a six-hole injector into a constant-volume chamber has been characterised, before and after fuel impingement on a hot surface simulating the piston in direct-injection gasoline engines, by means of spray visualisation and phase Doppler anemometry (PDA) measurements. Spray images have confirmed that penetration decreases with increasing chamber pressure or decreasing injection pressure, that higher droplet velocities are present at the spray centre and that a multi layer structure is formed along the spray axis. Stronger interaction between the six sprays is observed as the chamber pressure increases. The PDA measurements under both atmospheric and high pressure revealed that the mean droplet velocity prior to fuel impingement on the surface reaches its peak at the spray axis unlike the droplet mean diameter which exhibits an off-centre peak. The results also showed that the temporal variation of the mean droplet velocity at the spray centreline is similar to the predicted injection velocity variation at the nozzle exit while, further downstream and away from the centreline, three stages have been identified in the spray structure: leading edge, steady-state and tail. After the droplets impinge on the hot plate they move downstream forming a jet parallel to the plate surface with increasing or decreasing mean diameter depending on the surface inclination angle. The effect of injection pressure and ambient pressure/temperature on the droplet characteristics has been demonstrated and quantified.

1. Introduction

The competition amongst the automotive manufacturers to improve engine performance with minimum engine-out global and local emissions has driven intensive research on direct-injection spark-ignition (DISI) engines under development. Wide spacing and close spacing combustion systems have been introduced for DISI engines, depending on how close the spark plug is to the injector. In wide spacing wall-guided combustion systems, the spray which is injected late during compression impinges on the cavity of the purposely designed piston that guides the spray towards the spark plug just prior to ignition.

While the swirl-type injector has been fairly successful in the early wide spacing combustion configurations, it seems to fail in the close spacing system mainly due to the dynamic variations of the spray structure when the engine operating conditions change; this change in spray structure could cause engine misfire. Moreover the presence of large droplets in the pre-spray, causes an increase in the hydrocarbons emitted from the engine.

Recently, the spray structure from emerging new types of injector, such as multi-hole, slit, and outward opening pintle injectors, have been under investigation by many researchers. The use of a multi-hole injector has been examined at an early stage and compared with the swirl injector by Tomoda et al [1] who showed that the spray from the multi hole injector is more stable and repeatable, but has a relatively wide range of droplet size distribution. With the development of a similar injection system by Bosch, it became possible to increase the injection pressure beyond the range of operation of the swirl injector which allowed reduction of the bandwidth of droplet size distribution, as described by Ortman et al. [2]. The characteristics of the spray from a DISI multi hole injector have been investigated by Arndt et al. [3] and, more recently, by Mitroglou et al. [4] . They showed that the spray structure is not only stable under varying chamber thermodynamic conditions but that the droplet Sauter mean diameter is of the order of just 19-14 μm at injection pressure of 120 and 200 bar, respectively, with no evidence of large droplets such as those present in the pre-spray of swirl injectors. This type of injector has been employed successfully in Audi's 3.6 L V8 twin-turbo le Mans engine operating under homogeneous mixture conditions and based on a air guided combustion system, as described by Baretzky et al. [5]. In order to use this injector in the other types of combustion system, spray impingement on the hot piston/cylinder has to be studied. It has been reported by Stranglmier et al. [6] that impingement of the spray on the wall/piston is one of the major sources of HC emissions with a considerable percentage emitted during the engine cold start period according to Miller et al. [7].

Impingement of a single droplet on a hot surface has been investigated by many authors who have identified different droplet impingement regimes: stick (deposition), rebound, spread or splash (see for example, Bai and Gosman [8]). The impingement regimes were determined based on the incoming Weber number of the droplet and the impinging surface roughness and temperature. Although the spray consists of individual droplets, the behaviour of spray impingement is different from single droplet impingement due to the fact that the spray has high frequency of droplet impingement and different droplet sizes and velocities in addition to the different air-flow pattern near to the impingement area. Therefore, special attention has to be paid in order to take into account droplet-to-droplet interaction and droplet agglomeration, as well as the momentum exchange between the droplets and the airflow pattern. A liquid film may also be present on the surface after the impingement of some droplets in case the heat transfer rate from the surface is not fast enough to evaporate all the impinging droplets. Although different models have been introduced to characterise the spray before and after impingement on a surface, summarised by Lindgren et al. [9], most of these models are either based on single droplet or a chain of droplets. Very few studies have focused on real gasoline engine spray impingement.

The current study focuses on spray characteristics from a multi-hole injector before and after impingement on a hot surface simulating the piston. It is part of an experimental programme aiming to identify the parameters affecting the spray characteristics, combustion stability and engine-out emissions. These quantitative results have obtained in order to validate and develop further an in-house spray impingement model.

2. System description

A six-hole injector has been installed in a constant-volume chamber equipped with four quartz windows and connected to a pressurised nitrogen bottle that maintains the required pressure inside the chamber. An electrically heated plate has been fixed inside the constant volume chamber with a constant inclination angle and at a constant distance from the

injector of 31 mm, as shown in Figure 1. Using thermocouples, the temperature of the plate has been controlled by a closed loop temperature control unit. Three wall temperatures have been investigated: 381K, 435K and 489K. Only one spray out of six has been allowed to impinge on the hot polished surface inclined at two impinging angles of 60 and 30 degrees. The angle of impingement is calculated from the centreline of the spray plume to the line drawn normal to the impingement surface.

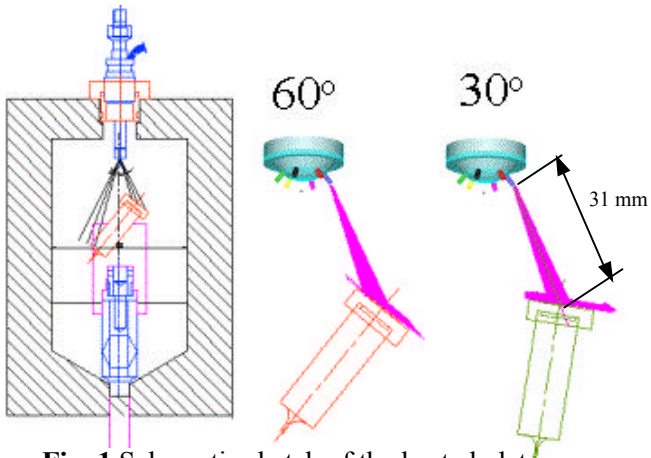

Fig. 1 Schematic sketch of the heated plate inside the constant volume chamber

For the purpose of spray imaging, a CCD camera and pulsed light have been synchronised with the injection pulses to allow imaging of the spray at different times from the triggering of the injection signal. In order to measure the droplet size and velocity at different locations within the spray, the PDA system has been aligned for a forward scattering angle of 70 degrees, as shown in Figure 2. The processor's coincidence mode has been used to simultaneously measure the axial/radial velocities and the diameter of the same droplet. Both the transmitting and the receiving optics have been installed on a PC controlled 3-D traverse mechanism moving relative to the constant volume chamber.

Measurements have been obtained for two-injection pressures of 70 bar and 100bar, three chamber pressures of 1, 3 and 7bars and the above three wall temperatures with an injection frequency of 0.25 injection/second. Data has been collected within a time window of 0.2 ms and for up to 7 ms from the start of the injection signal. Measurements have firstly been obtained for the free spray without impingement, starting from the centre and up to 30 mm in the axial direction, and in a direction perpendicular to the spray centreline with a 2 mm step until the spray edge. Having completed the free spray measurements, the heated plate was re-installed and the new measurements points were located parallel to the wall surface with a step of 2mm at three planes 1, 3 and 5 mm above the plate, as shown in Figure 3. The fuel used in this study is Iso-Octane (trade name 2,2,4 Trimethylpentane 99.7 % HPLC grade), which has similar properties to gasoline but is safer in use and, in addition, it is a single component fuel with a boiling temperature of 99°C and specific gravity of 0.69, thus making it easier to validate the mathematical model.

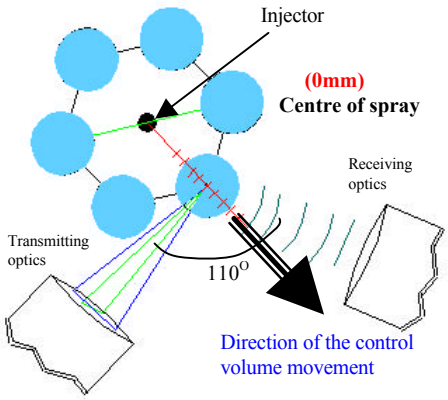

Fig. 2 Layout of the PDA transmitting optics relative to the spray and the measurement points

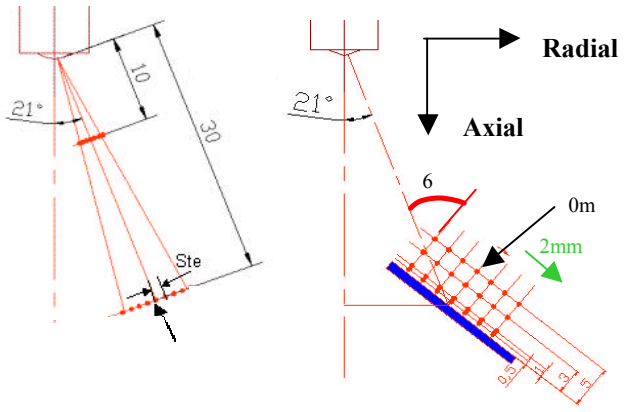

Fig. 3 Location of the measurement points relative to the hot plate and the injector

3. Spray Visualisation Results

Prior to spray imaging, the time duration from the initiation of the injection signal to the first appearance of fuel at the nozzle exit was estimated to be 0.65 ms while the time to the end of injection was 1.9 ms. Accordingly, for a demand injection duration of 1.5 ms, the actual injection duration is 1.25 ms. Images were then collected at different times from the start of fuel appearance at the nozzle exit for different injection and chamber pressures. These images have shown that the interaction among the six sprays becomes more significant as injection pressure increases, according to Figure 4. These images also showed that the spray angle remains constant while the tip penetration increases with increasing injection pressure; penetration increases until it reaches an asymptotic value as shown in Figure 5.

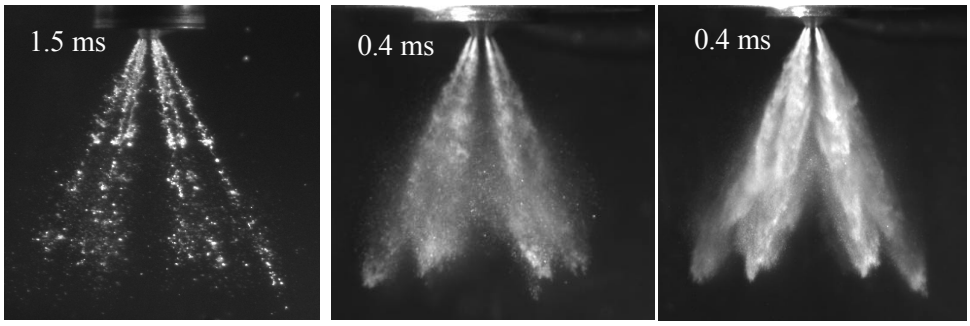

Fig. 4 Spray images at different injection pressures and times for the same spray penetration.

In order to minimize the effect of spray interaction on the characterisation of the spray during its impingement on a hot surface, the plate simulating the piston has been heated to the required temperature and positioned so that it encounters only one out of the six sprays. PDA measurements have been obtained only along the centreline of the spray cross section to avoid any influence from nearby sprays. Images of the spray near the plate for an impingement angle of 60 degrees are shown in Figure 6. These images confirm that, as the spray hits the plate, the droplets move forward as a wall jet along the plate surface with a possibility of droplet agglomeration, splashing or deposition. Spray impingement at a 60 degree incidence angle has lower impact velocity (velocity normal to the wall surface); thus the reflected or splashed droplets have even lower normal velocities. In this case agglomeration of the droplets seems to be more dominant, as the wall jet travels along the plate, than the 30 degree incidence angle and this is clear in the images of the spray after impingement shown in Figure 6.

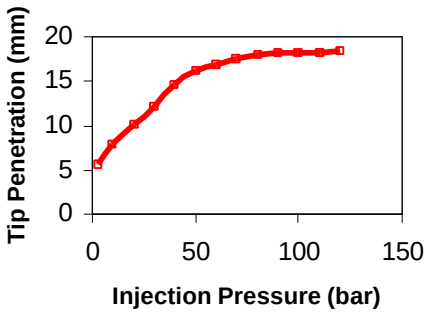

Fig. 5 Effect of injection pressure on spray penetration

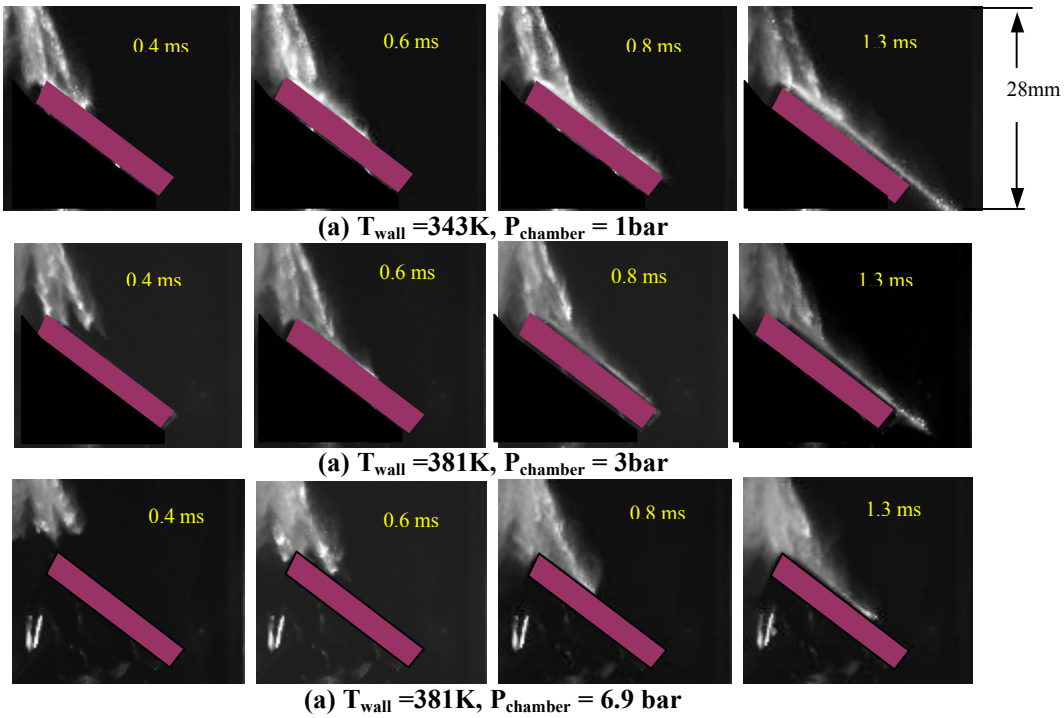

Fig. 6 Impinging spray development at different chamber pressures and elevated wall temperatures (for the 60 degrees inclination angle).

4. PDA measurements

4.1 Before Impingement (Free spray)

The temporal variation of the droplet mean velocity at 30mm away from the nozzle hole exit along the spray centre line is presented in Figure 7. Figure 7a shows the scattered plot of the axial velocity and the arithmetic mean value during the injection duration while Figure 7b shows the temporal variation of the mean velocity, the mean diameter and the mean travelling angle at the same location but for different injection and chamber pressures. Away from the spray centre line the temporal variation of the mean droplet velocity could be divided into three stages: leading edge, steady state and tail. The leading edge represents the first group of droplets arriving at the control volume which have relatively large size and are less decelerated by the aerodynamic forces. During the steady stage there is a band of droplet velocities, however their mean value does not change considerably; the same applies to the mean droplet diameter. The tail of the spray includes those droplets arriving at the control volume after the needle closes which have lower velocity due to the loss of their momentum and the absence of any following droplets pushing the flow in the direction of the mean droplet motion. Therefore, the drag forces on these late arriving droplets are expected to be high and their velocities much lower.

Increasing the injection pressure from 70 to 100bar almost doubles the mean droplet velocity with a reduction in the droplet mean diameter due to the enhancement of the primary atomisation process and secondary droplet break-up. On the other hand, an increase in the ambient pressure causes a reduction in the droplet velocities which increases the chances of droplet agglomeration and lead to an increase in the mean droplet diameter, as shown in Figure 7. This figure also shows that the mean droplet penetration angle, which is calculated based on the travelling angle of the individual droplets, remains constant and independent of injection and chamber pressure. This provides additional

confirmation, besides spray visualization, about the stability and repeatability of the sprays injected from multi hole atomizers independent of injection and ambient pressure.

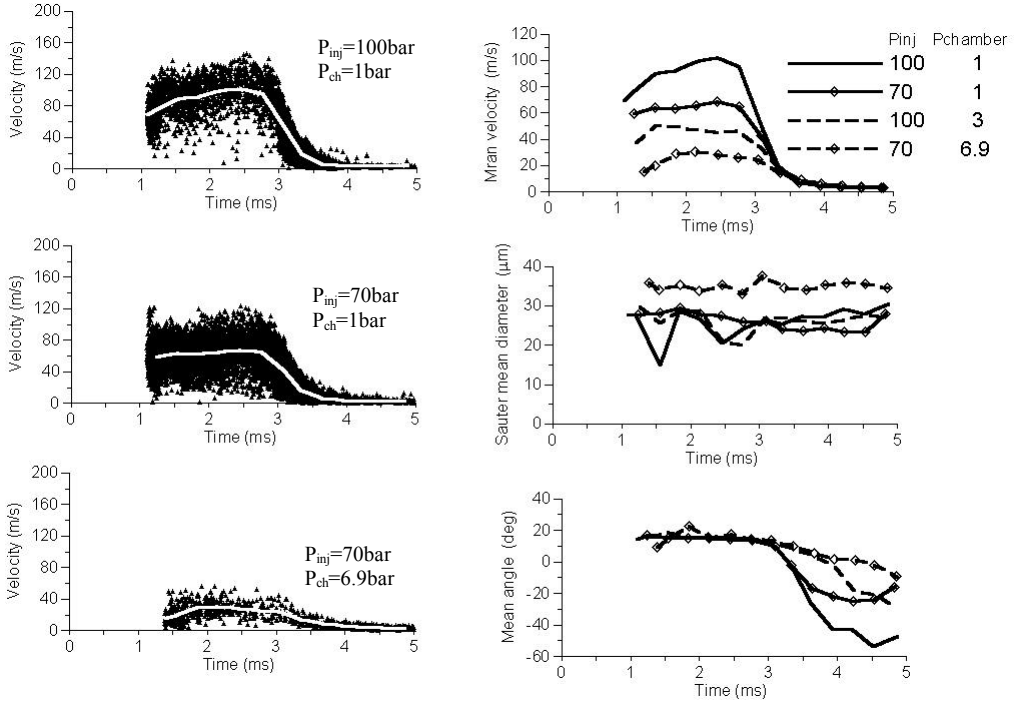

Fig. 7 Mean droplet velocity, diameter and direction at different injection and chamber pressures, at 30 mm away from the nozzle exit on the spray centreline

The spatial distribution of the mean droplet velocity across the spray shows that droplets located close to the spray centre line move faster than droplets located towards the edge of the spray, according to Figure 8. On the contrary, the mean droplet diameter has its minimum value at the spray centreline where the highest velocities have been recorded. The presence of large droplets away from the spray centre line could possibly be attributed to the coalescence of droplets as a result of the relatively lower droplet velocities and air entrainment at the spray edges.

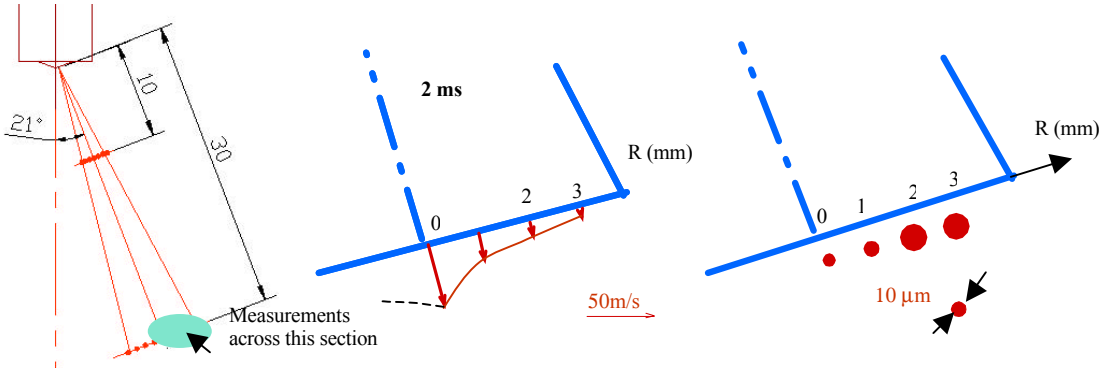

Fig. 8 Mean droplet velocity and diameter across the spray at 30 mm away from the nozzle exit, 100bar injection pressure and 3bar chamber pressure after 2ms from the start of injection

4.2 Impinging spray

60 degree impinging angle

Spray images have revealed that after the spray hits the plate, it moves as a wall jet parallel to the plate. PDA measurements obtained 1mm above the plate have shown that the droplet mean diameter increases, after impingement on the hot surface, as they travel along the plate according to Figure 9. In order to explain the reason for that increase in the mean diameter, the direction of each individual droplet arriving at the control volume has been calculated from the measured axial and radial velocity during spray impingement. A wide spectrum of the droplet travelling directions has been observed at two points. Figure 10 shows the frequency of the droplets direction at two positions located 1 mm above the plate surface and at 4mm and 8mm away from the spray centre line. This figure shows that the droplets arrive at the control volume after impingement from different directions and therefore the possibility of collisions is very high. Accordingly, droplets arriving at the

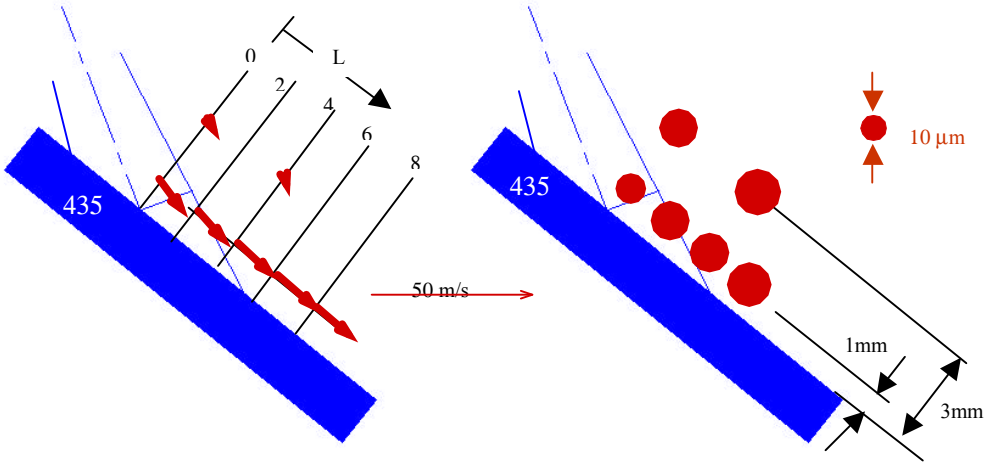

Fig. 9 Mean droplet velocity and diameter variation along the hot plate (435 K) after impingement after 3ms from start of injection for 60 degree impingement angle

control volume could be classified into two classes depending on their direction. The first class is the main jet, which contains the droplets arriving at the control volume within a narrow angle relative to the plate inclination angle. The second class contains droplets having very different directions, as a result of either bouncing or secondary break-up and collisions. Although the droplets arrive to a specific location from different directions, the mean velocity of the droplets is almost parallel to the plate surface, as shown in Figure 9.

The temporal variation of the droplet mean velocity after impingement shows similar stages to those described for the free spray but with relatively lower mean velocity

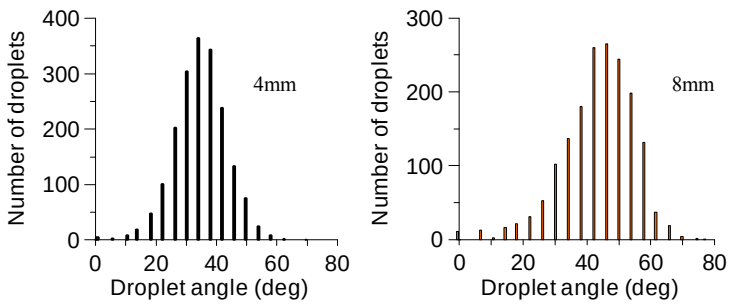

Fig. 10 Distribution of droplet travelling angles as they reach the control volume 1mm above the plate for 4mm and 8mm away from the spray centreline

according to Figure 11a. The temporal variation of the droplet mean diameter slightly decreases with time and that decrease has been noticed for all operating conditions, as shown in Figure 11b. Increasing the wall temperature results in a slight increase in the mean droplet velocity. This increase becomes more significant as the droplets move downwards along the hot plate after impingement; there is also a slight decrease in the mean diameter.

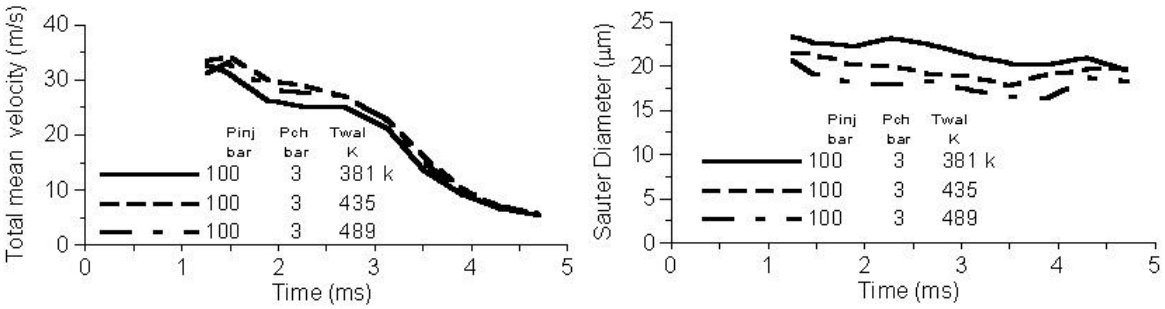

Fig. 11 Temporal variation of droplet mean velocity and Sauter mean diameter at different wall temperatures at 1 mm above the plate and 4 mm distance away from the spray centreline

30 degree impinging angle

Unlike the 60 degree impingement angle, the PDA measurements parallel to the plate for the 30 degree impingement angle showed that the droplet mean diameter decreases after impingement, as the droplets travel away from the impingement area along the heated surface (Figure 12). This observation implies that the design of the piston bowl, especially around the impingement angle, can have a significant effect on the secondary droplet sizes after impingement. Spray images and PDA measurements confirm that the droplets after impingement are reflected into a jet which then reaches a stagnation point before starting to form a counter rotating vortex of droplets, as shown in Figure 13. A significant number of droplets have contributed to the measurements at 3 mm and 5 mm above the plate while, for the 60 degree inclination angle, measurements were only possible at 1 mm above the plate as the data rate was very low due to the low number of droplets. This implies that for the 60 degree impinging angle, only a jet is produced and no counter vortex seems to be formed as confirmed by the images shown previously in Figure 6

Although figure 13 reveals that at 1.3 ms droplets are reflected after impingement, later at 2 ms a jet parallel to the plate is evident at 1mm away from the surface which moves steadily. The recirculation of the droplets continued even after the end of injection and large droplet sizes are observed after impingement which could be attributed to droplet agglomeration which is more likely for the low velocity moving droplets.

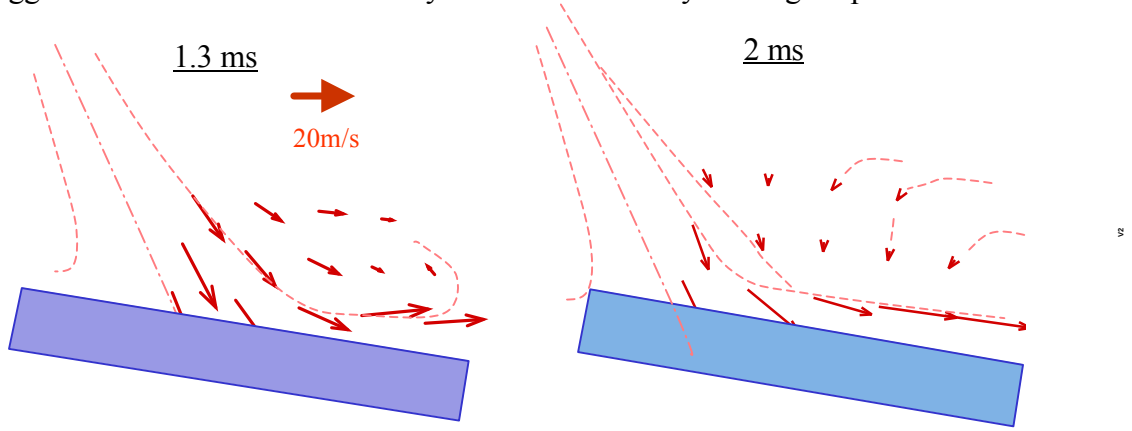

Fig. 13 Spatial distribution of droplet mean velocity after impingement on a hot surface of 435 K for 30 deg. impingement angle under 100 bar injection pressure and 3 bar chamber pressure

5. Conclusions

Spray images and PDA measurements obtained for both a free and an impinging spray on a hot surface have showed that the spray from a multi hole injector maintains a constant angle independent of injection or chamber pressure. The results for the free spray also showed that the mean velocity of the droplets across the spray exhibits its maximum value at the spray centreline where the droplet diameter is minimum. The droplet mean diameter after impingement has been found to be strongly dependent on the plate inclination angle. A wall jet has been created after impingement on the hot surface without a subsequent recirculation zone when the impingement angle is too large. Increasing the surface temperature of the plate leads to a slight increase in the mean velocity of the droplets after impingement and a decrease in their Sauter mean diameter.

6. Acknowledgement

The authors would like to thank Dr. J. Nouri, N. Mitroglou and J. Ford for their contribution to the design and construction of the injection system and the constant volume chamber.

7. References

[1] **Tomoda T, Sasaki S, Sawada D, Saito A, and Sami H 1997**. *SAE* 970539.
[2] **Ortmann R, Arndt S, Raimann J, Grzeszik R and Wurfel, G 2001** *SAE* 2001-01-0970
[3] Arndt S, Gartung K and Bruggemann D 2001 *Proc. ILASS-Europe 2001*
[4] Mitroglou N, Nouri J M and Arcoumanis C, *Proc. ICOLAD - 2002*
[5] Baretzky U, Andor T, Diel, H and Ullrich W 2002 *SAE* 2002-013357
[6] Stanglmaier R H, Li J and Matthews R D 1999 *SAE* 1999-01-0502
[7] Miller A L, Ginter D, Seaba J P, Loyalka S K and Ghosh, T K 1998 *IMechE*, **Vol. 212 Part D, pp 525-532**
[8] **Bai C and Gosman A D 1995** *SAE* **950283**
[9] Lindgren, R and Denbratt, **I** *SAE* **2000-01-2808**